Hindawi
Journal of Food Biochemistry
Volume 2023, Article ID 7499169, 13 pages
https://doi.org/10.1155/2023/7499169

Research Article

A Comparative Analysis of the Flavor, Aroma, and Compositions in Three Levels of Stir-Frying *Cyperus rotundus* Using E-Tongue, E-Nose, and HS-GC-MS

Fengxia Wang,[1] **Qi Qian**,[1,2,3] **Hanyu Ma**,[1] **Yu Feng**,[1] **Jingnan Hu**,[1] **Baolin Li**,[1,2,3] **Liying Niu**,[1,2,3] **and Xinguo Wang**[1,2,3]

[1]*School of Integrated Traditional Chinese and Western Medicine, Hebei University of Chinese Medicine, Shijiazhuang, Hebei, China*
[2]*Hebei Traditional Chinese Medicine Formula Granule Engineering and Technology Innovate Center, Shijiazhuang, China*
[3]*Quality Evaluation and Standardization Hebei Province Engineering Research Center of Traditional Chinese Medicine, Shijiazhuang, China*

Correspondence should be addressed to Liying Niu; niuliyingyy@163.com and Xinguo Wang; wangxinguozy@163.com

Received 30 December 2022; Revised 13 June 2023; Accepted 26 June 2023; Published 13 July 2023

Academic Editor: Anand Babu Perumal

Copyright © 2023 Fengxia Wang et al. This is an open access article distributed under the Creative Commons Attribution License, which permits unrestricted use, distribution, and reproduction in any medium, provided the original work is properly cited.

Cyperus rotundus (CR) is the dry rhizome of the *Cyperaceae* plant *Cyperus*, which is widely used in food processing, such as curry, pickling spices, and baking goods, as well as medicinally after stir-frying. The level of stir-frying (slightly stir-frying, stir-frying yellow, and stir-frying black) has a direct impact on the flavor, aroma, and pharmacological effects of the food. However, the distinctions between various levels of stir-frying have not been studied. The purpose of this study was to develop a method that combines electronic tongue, electronic nose, and HS-GC-MS to elucidate the flavor and aroma differences between three types of stir-fried CR and to identify aroma difference components. As the degree of stir-frying increased, the sweet, bitter, astringent, and umami flavors of the sf-CR diminished while the aroma intensified. Among the 33 differential compounds, pyrazines, D-limonene, camphene, trans-verbenol, and ponocarvone were the most significant aroma-causing components. This method effectively differentiates the three levels of sf-CR and provides a foundation for the use of sf-CR in food processing and pharmaceutical applications.

1. Introduction

Cyperus rotundus (CR, known as Xiang Fu in Chinese), the dried rhizome of *Cyperus rotundus* L., is highly valued as both food and medicine [1]. In clinical practice, it is frequently prescribed for abdominal distention, irregular menstruation caused by liver depression, blood deficiency and qi stagnation, irregular menstruation, chest, and abdominal pain [2]. In addition, it is a raw material for curry, salted spices, Greek dishes, and baked goods [3].

Stir-frying is one of the CR processing methods that have been used in China for more than 1340 years [4]. Throughout history, there have been primarily three levels of stir-frying: "slightly stir-frying," "stir-frying yellow," and "stir-frying black" [5–7]. However, relatively few studies have been conducted on stir-fried foods. Until now, the differences between them have been unknown, preventing the full exploitation and application of sf-CR in food and TCM prescriptions. Thus, new research into three distinct levels of sf-CR is required.

Research on the processing mechanism is the foundation of food and traditional Chinese medicine (TCM) processing, as well as the key to TCM's internationalization and modernization. CR contains numerous chemical components that act on various pharmacological targets and regulate numerous biological mechanisms [8]. Consequently, only one or a few of the constituents provide a comprehensive explanation of their processing

mechanism. Chemical component analysis has been increasingly applied to identify food and TCM [9]. Metabolomics is among the emerging "-omics" technologies [10]. It is consistent with the overall theory of Chinese medicine and may provide a novel approach to revealing the processing mechanism [11]. To date, numerous experimental studies on volatile components (VOCs) and the pharmacological effects of CR have been published. Accordingly, VOCs are believed to be the primary active components of CR. It is established that volatile components are one of the primary active components in CR [12, 13]. Therefore, comparing VOCs for the three stages of sf-CR stands highly relevant. Several extraction techniques (carbon dioxide, supercritical fluid extraction, and hydro-distillation) have been reported [14–16] as essential steps in the analysis of volatile organic compounds (VOCs). However, the majority of these methods are time- and resource-consuming. In this regard, gas chromatography–mass spectrometry (GC-MS) comprises a direct and rapid approach to the identification of VOCs. In addition, headspace (HS) sampling has been demonstrated to be a rapid, simple, and convenient method for VOC analysis. HS-GC-MS combines the advantages of HS and GC-MS in terms of speed, convenience, and sensitivity and has, therefore, emerged as a potent instrument for analyzing VOCs.

Previous research in long-term medical practice has established a connection between TCM flavor and aroma and its pharmacological effects [17]. According to modern medicine, the difference between the flavor and aroma of TCM is a direct result of its chemical composition [18]. Therefore, evaluating the intrinsic properties of decoction pieces via flavor can provide new perspectives and references for the prescription and clinical application of Chinese medical decoction [19]. The evaluation of "flavor and aroma" is gradually shifting from artificial subjective feeling to digital and visual evaluation as a result of the continuous development of modern analysis technologies. The advancement of bionic technologies, such as the electronic tongue and electronic nose, not only provides a tool for defining the flavor and aroma of traditional Chinese medicine but also introduces new research methodologies to explain the mechanism of processing decoction pieces [20–22]. Currently, E-tongue and E-nose technologies are utilized extensively in the food, TCM, agricultural detection, and environmental monitoring industries [23–27]. However, no report exists to date on the use of the E-tongue and E-nose systems to evaluate the flavor of CR.

Therefore, in the present study, we developed a method that efficiently combines plant metabolomics, network pharmacology, and sensory bionic technology to investigate the changes in CR before and after vinegar processing. Using HS-GC-MS and a data analysis strategy based on metabolomics, we then screened, identified, and compared the major volatile compositional differences between RCR and VCR. Finally, the differences in aroma between the three types of sf-CR were explained using Spearman's rank correlation between aroma and volatile compounds. The findings are expected to clarify the changes in flavor, aroma, and volatile components of CR during stir-frying, as well as the process mechanism, in order to lay a foundation for its application in foods and formulations.

2. Materials and Methods

2.1. Reagents and Materials. Tartaric acid (analytical grade) was purchased from Tianjin Oberkai Chemical Co., Ltd., whereas potassium chloride (analytical grade) was procured from Tianjin Best Chemical Co., Ltd. Deionized water used in the study was obtained used a ULUPURE series ultrapure water machine (Model: UPR-II-20L). In addition, positively and negatively charged membrane washing solutions were purchased from Beijing Ying Sheng Heng Tai Technology Co., while the internal solution (211119) was procured from Beijing Ying Sheng Heng Tai Technology Co. Methanol of HPLC grade was attained from Fisher Scientific (Fair Lawn, NJ, USA); cyperotundone (DST201120-156, 98%) and α-cyperone (DST200819-022).

2.2. Sample Collection and Processing. Ten batches of raw *Cyperus rotundus* were collected from the Anguo medicinal materials market in Hebei province, which were authenticated by the Chief Chinese pharmacist Jiping Duan (Hebei Institute of Drug and Medical Device Control). The voucher specimens were then deposited at the Hebei Traditional Chinese Medicine Formula Granule Engineering and Technology Innovate Center, Shijiazhuang, China. These 10 batches of raw-RC were subsequently utilized to prepare 30 batches of sf-CR. The batches were categorized as follows: (a) slightly stir-fried (LY1-LY10)—raw-RC granules were slightly stir-fried over a mild fire for 5 min until the surface turned light yellow in color; (b) stir-frying yellow (Y1–Y10)—raw-RC granules were stir-fried over a mild fire for 15 min until the surface turned yellow in color; (c) stir-frying black (B1–B10)—raw-RC granules were stir-fried over a mild fire for 30 min until the surface turned dark brown in color. All samples were dried at room temperature and crushed to obtain a particle size between 50 ($355 \pm 13\,\mu$m) and 80 meshes ($180 \pm 7.6\,\mu$m).

2.3. E-Tongue System and Sampling Procedure. The E-tongue (SA402B, INSENT, Japan) consisted of a sensor array, special beakers, signal acquisition, and data analysis software packages and was used to detect the flavor. The sensor array consisted of 6 sensors (AAE, CTO, CAO, COO, AE1, and GL1) that were sensitive to the umami, salty, sour, bitter, astringent, and sweet flavors, respectively. The sensor unit measured the reference solution for 30 s, and at the conclusion of the measurement, the electrical potential was recorded. The detector unit then measured the sample solution in a similar manner. After measuring the sample solution, the sensor unit was briefly rinsed in the stock solution, and the reference solution is remeasured for 30 s using the detector unit. The sensor unit was finally washed with the wash solution and flushed with the reference solution for subsequent measurements.

1.0 g of the sample was collected and placed in a conical vial (100 mL) equipped with a stopper. Then, 100 mL of pure water was added with sonicating for 30 minutes. The resultant mixture was then added to a 100 mL centrifuge tube and centrifuged for 10 min at 4000 rpm•min^{-1}. A special beaker was then used to test ~35 mL of the as-obtained supernatant. Finally, four replicates of the sample were analyzed, and the raw data from the last three replicates were selected for analysis [28].

2.4. E-Nose System and Sampling Procedure. The aroma of sf-CR was evaluated using a PEN3.5 portable E-nose (Air sense Analytics GmbH, Schwerin, Germany) equipped with 10 sensors: W1C, W5S, W3C, W6S, W5C, W1S, W1W, W2S, W2W, and W3S. Table 1 illustrates the performance of these 10 sensors [19].

1.0 g of the samples were measured and placed in a 100 ml glass beaker. The samples were then sealed using two layers of sealing film and allowed to rest at room temperature for 30 min to ensure that the sample aroma was acceptable and that its test procedure was equilibrated under the following conditions: flush duration—120 s; sample interval—1 s; zero-point trim time—10 s; presampling time—5 s; measurement time—120 s; and gas flow rate—600 mL•min^{-1} [29, 30]. Each sample was analyzed in triplicate.

2.5. Analysis of Volatile Compounds Using HS-GC–MS

2.5.1. HS-GC-MS Conditions. The headspace injection conditions were as follows: a 20 mL headspace inlet vial containing 0.5 g of sf-CR powder was sealed and incubated at 120°C for 30 min.

The gas chromatography conditions are outlined as follows: volatile components of sf-CR samples were analyzed using a GC 2030 gas chromatograph (Shimadzu, Japan). The volatile components were isolated on an SH-I-5SiI MS (30 m × 0.25 mm × 0.25 μm, Shimadzu, Japan). The temperature program began at 50°C; it was then raised to 70°C at a rate of 2°C/min. Subsequently, it was raised to 120°C at a rate of 10°C/min, following which it was raised to 210°C at a rate of 5°C/min and maintained for an additional 2 min. The carrier gas comprised helium (purity 99.99%) with a constant flow rate of 1.5 mL/min. The injection volume was 1 μL with 1 : 20 splits.

The mass spectrometry conditions were as follows: MS detection was carried out on a TQ8050 NX mass spectrometer (Shimadzu, Japan). The ion source temperature was 230°C, while the interface temperature was 250°C. In addition, a mass scan range of 50–600 m/z was utilized, while the solvent delay was maintained at 2.5 min.

2.5.2. Quality Control Measurement. Quality control (QC) samples were obtained by mixing 0.5 g of each sample in order to validate the repeatability and stability of the assay system. A total of eight consecutive QC samples were tested to evaluate the stability and reliability of the system and methods. During the formal testing process, every fifth sample is interspersed with a QC sample to assess repeatability and precision.

2.6. Data Analysis. The statistical analysis was conducted using the Statistical Package for Social Sciences 19.0 (SPSS Inc., Chicago, IL, USA). SIMCA-P14.1 (Umetrics AB, Umea, Sweden), GraphPad prism (8.0, San Diego, California, USA), and ChiPlot Online platform (https://www.chiplot.online/) were utilized for the statistical analyses (PCA, OPLS-DA, HCA, and group error bar plot) [31]. For peak extraction, MS-DIAL 4.90 was used [32]. VIP (OPLS-DA) was obtained using SIMCA-P14, while P value (T-test) and FC (fold change) were obtained using Excel [33]. Finally, VIP > 1, $P < 0.05$, and FC ≥ 2 or FC ≤ 0.5 as the threshold was used to obtain the differential compounds [34–36]. The total differential compounds are the union of three differential compounds. The identification of differential compounds was performed using NIST 20.0 database and retention indexes (RI) [37]. First, we matched the experimental data with the database, including RI, secondary mass spectrometry fragments, and similarity parameters. The obtained mass spectrum is compared with the known compounds in the database to determine the name, molecular formula, and other information of the compounds. Then, the obtained ingredient information is verified with the information reported in the literature.

3. Results and Discussion

3.1. E-Tongue Analysis. The output value generated by the reference solution was 0. Except for sourness and saltiness, every other indicator had a flavorless value of 0. Furthermore, the flavorless points for sourness and saltiness were −13 and −6, respectively, because the reference solution was composed of potassium chloride and tartaric acid, which contain a small quantity of acid and salt [38, 39]. Figure 1(a) demonstrates that the saltiness and sourness of the samples fall below the criterion for flavorlessness. Additionally, astringency, aftertaste, and richness had values that were close to the flavorless point, whereas bitterness, umami, and sweetness had values that were significantly greater than the flavorless point (Table S1). Subsequently, we examined various effective indicators after removing the saltiness and sourness values.

Based on the principal component analysis (Figure 1(b)), the first principal component (explaining 58.3% of the variance) distinguished light stir-frying from yellow and black, whereas the second principal component (explaining 20.7% of the variance) distinguished stir-frying yellow from black. Correspondingly, the results demonstrated significant differences in flavor between groups, with the greatest difference between the light stir-frying group and the other two groups, in addition to a relatively small difference between the yellow and black groups. Hierarchical clustering analysis (HCA) is a statistical technique for identifying relatively homogeneous sample groups based on particular

Table 1: Sensors and their main sensitive substances of PEN3.5 E-nose.

Number	Sensor name	Mainly sensitive substance	Sensitivity (mL·m^{-3})
1	W1C	Aromatic compounds	10
2	W5S	Nitrogen oxides	1
3	W3C	Ammonia and aromatic compounds	10
4	W6S	Hydrogen	100
5	W5C	Alkenes and aromatic compounds	1
6	W1S	Methane	100
7	W1W	Terpene, sulfides compounds	1
8	W2S	Alcohols, partially aromatic compounds	100
9	W2W	Aromatic compounds and organic sulfides	1
10	W3S	Alkenes	10

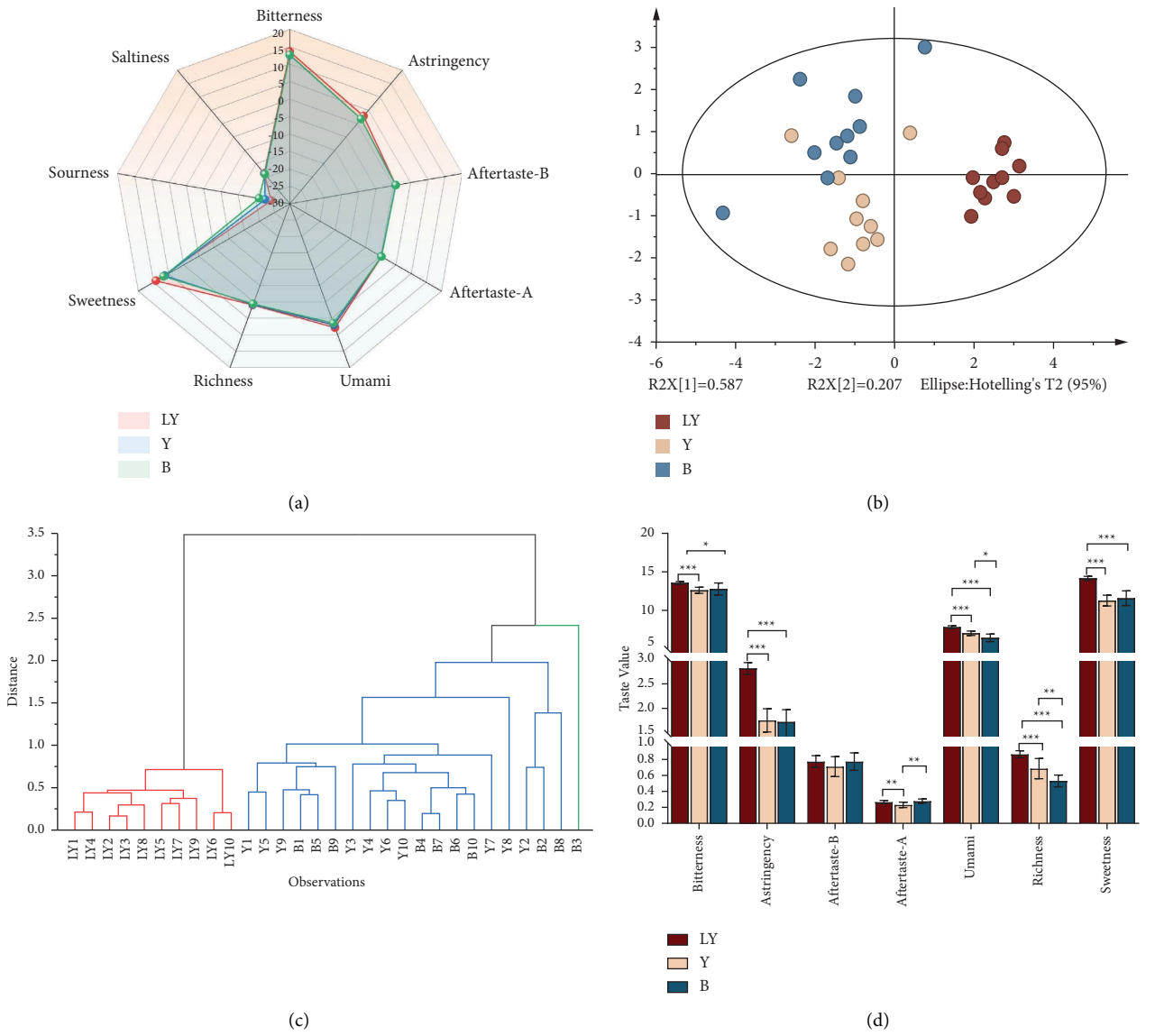


Figure 1: Comparison of flavor with different levels of sf-CR: radar plot (a), principal component analysis score plot (b), HCA dendrogram (c), and group error histogram (d) for flavor information. (The symbol "∗" represents the significance of the difference, and numbers 1 to 3 represent $P < 0.05$, 0.01, and 0.001, respectively).

characteristics [40]. Figure 1(c) depicts the flavor HCA for each sample, wherein the horizontal axis represents the sample, and the vertical axis represents the distance. Correspondingly, sf-CR samples were divided into two clusters: one for yellow and black stir-frying and the other for light stir-frying. As observed, the findings were consistent with the principal component analyses (PCA) results mentioned previously.

A one-way ANOVA was conducted to gain additional insight into the flavor that contributed to the aforementioned differences (Figure 1(d)). Except for aftertaste-B (bitterness aftertaste), a significant difference in the sf-CR for six of the seven flavors was observed. The response values for sweetness, bitterness, astringency, umami, and richness were significantly greater in the slightly sf-CR than in the yellow and black ones ($P < 0.05$). Additionally, the stir-frying yellow and black groups differed significantly only in aftertaste-A (astringent aftertaste), umami, and richness ($P < 0.05$), whereas there was no significant difference in sweetness, bitterness, and aftertaste-B. Overall, the flavor of CR decreased as stir-frying grades increased.

3.2. E-Nose Analysis. The average response values of E-nose sensors for each sample are provided in Table S2. Compared to other sensors, the W5S, W2W, and W1W exhibited a significantly larger magnitude of response to each sample. Correspondingly, the difference between the three sf-CR groups was investigated using univariable and multivariable analyses.

The distribution of the PCA score plot (Figure 2(a)) revealed that the stir-frying lightly, yellow, and black groups exhibited distinct clustering. Furthermore, the yellow stir-fry group was much closer to the light stir-fry group than the black group, implying that the more intense the stir-frying, the greater the aroma change. In addition, the variance contribution rate of the first principal component PC1 was 47.1%, and the variance contribution rate of the second principal component PC2 was 19.1%; cumulatively, they accounted for 66.2% of the information in the original data set cumulatively. When combined with the loading plot (Figure 2(b)), sensors W1S and W6S contributed the most to the first principal component, followed by sensors W2W and W1W. Additionally, sensor W2S made the greatest contribution to the second principal component. Similar comparisons were also performed using hierarchical clustering analyses with very similar outcomes (Figure 2(c)). Correspondingly, the 30 batch samples were divided into 3 major clusters: slightly stir-fried, yellow, and black, respectively. Both principal component analysis and hierarchical clustering analyses revealed statistically significant differences between the three sample groups.

A one-way ANOVA was conducted to learn more about the aroma responsible for the aforementioned differences; the results are depicted in Figure 2(d). Six of the ten sensors, excluding W1C, W3C, W5C, and W3S, exhibited a significant variation in sf-CR. This may be the primary reason for the differences between the three sf-CR groups. As shown in Table 1, the content of nitrogen oxides, hydrogen, metal, terpene, and aromatic compounds differed significantly between the three groups of sf-CR. In addition, the yellow and black stir-fry samples had a stronger aroma than the light stir-fry samples ($P < 0.05$); in particular, the difference in aroma associated with W6S, W1W, and W2W was significantly stronger ($P < 0.01$). The combination of W5S, W6S, W1S, W1W, and W2W was primarily responsible for the negligible differences in aroma between stir-fried yellow and black CR samples ($P < 0.05$). Moreover, the W1W sensor aroma of black stir-fry samples were less than that of yellow samples, while the aroma of all other samples increased, with the W1S and W2S enhancement tendencies being more significant ($P < 0.01$). In conclusion, as the stir-frying grade increased, the aroma of CR steadily increased.

Modern chemistry recognizes flavor as one of the predominant sensory properties. Multiple compounds interact intricately to produce flavor and aroma. Since flavor and aroma are chemosensory parameters, the senses are just as important as the chemical components [41]. The E-tongue and E-nose closely mimic the perception and evaluation of flavor and aroma by the human tongue and nose and objectively evaluate them [42, 43].

3.3. HS-GC-MS Analysis

3.3.1. Screening of Differential Compounds. As depicted in the PCA plot (Figure 3(a)), QC samples clustered together, indicating that the instrument was stable, and the method was repeatable. PCA analysis revealed that 30 batches of SF-CR samples were separated into three groups: lightly stir-fried, yellow, and black, indicating that VOCs varied among the three groups to identify the differential VOCs responsible for the differences in sf-CR. We first performed a preliminary screening of the potential differential VOCs based on $P < 0.05$ and FC ≥ 2 or ≤ 0.05, and we visualized the screening results using volcano plots. A total of 38 potential differential compounds (3 upregulated and 35 downregulated) were identified between the yellow stir-fried and lightly stir-fried CR samples (Figure 3(b)); in addition, 94 potential differential compounds (48 upregulated and 56 downregulated) were identified between the lightly stir-fried lightly and black stir-fried CR samples (Figure 3(c)), and 56 potential differential compounds (20 upregulated and 36 downregulated) were identified between the stir-fried yellow and stir-fried black CR samples (Figure 3(d)).

OPLS-DA is a method of multivariate statistical analysis with supervised pattern recognition that can effectively filter out differential VOCs by removing irrelevant influences from the search [44]. As depicted by the OPLS-DA scatter plot (Figures 4(a), 4(d), and 4(g)), pairs of samples from the stir-frying lightly, yellow, and black groups were more easily distinguished more clearly in pairs, as shown in the OPLS-DA scatter plot (Figures 4(a), 4(d), and 4(g)). Figures 4(b), 4(e), and 4(h) depict the results of a permutation test that demonstrated the model's strong predictive accuracy and stability. The VOCs with VIP >1 are shown in Figures 4(c), 4(i), and 4(f) (red dot). Finally, the differential VOCs with $P < 0.05$, FC ≥ 2 or ≤ 0.05, and VIP >1.0 were

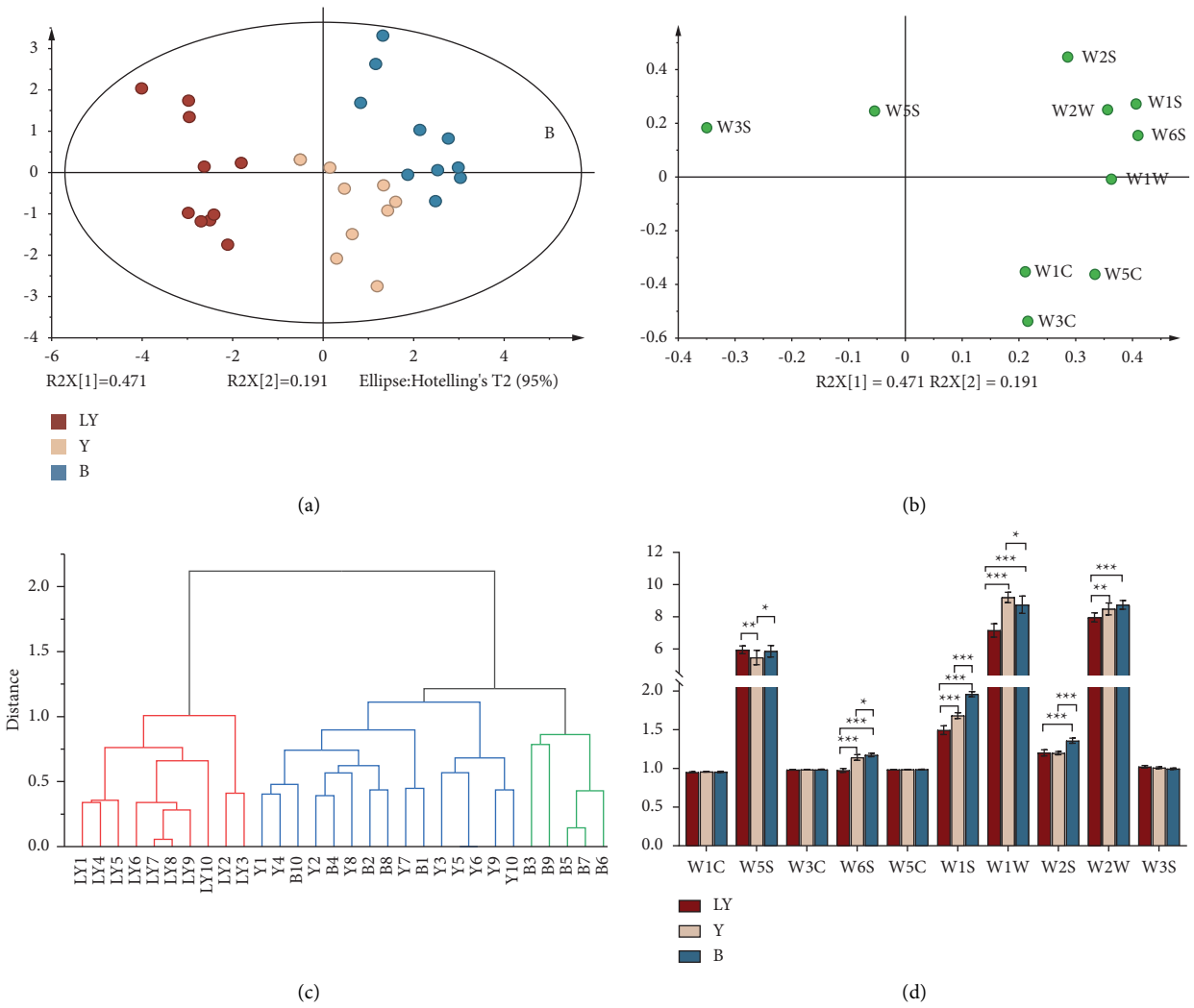


Figure 2: Comparison of the aroma of different levels of sf-CR: principal component analysis score plot (a) and loading plot (b), HCA dendrogram (c), and group error histogram (d) for aroma information. (The symbol "∗" represents the significance of the difference, and numbers 1 to 3 represent $P < 0.05$, 0.01, and 0.001, respectively).

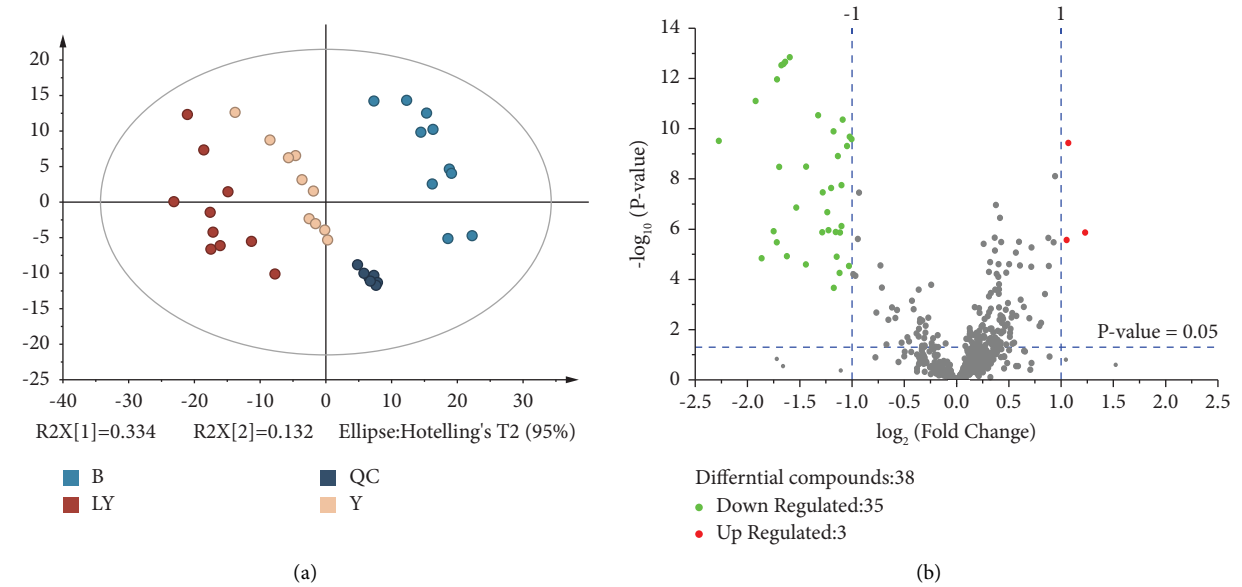


Figure 3: Continued.

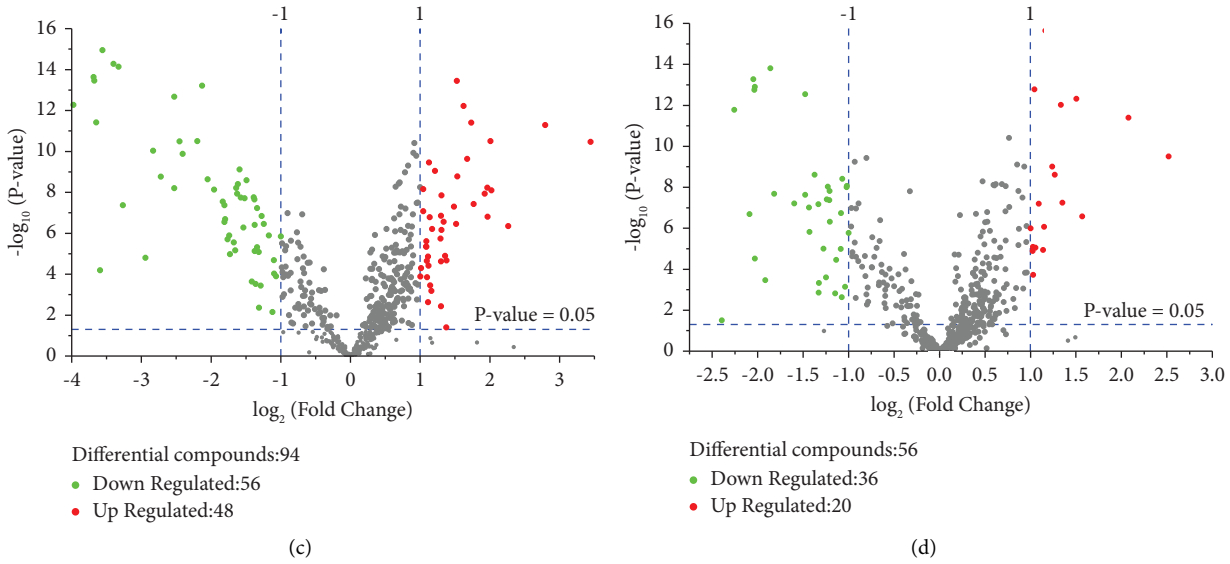


Figure 3: Multivariate statistical analysis of metabolic profiles derived from various sf-CR samples: PCA score plot (a) and volcano plots: (b) LY vs. Y; (c) LY vs. B; (d) Y vs. B.

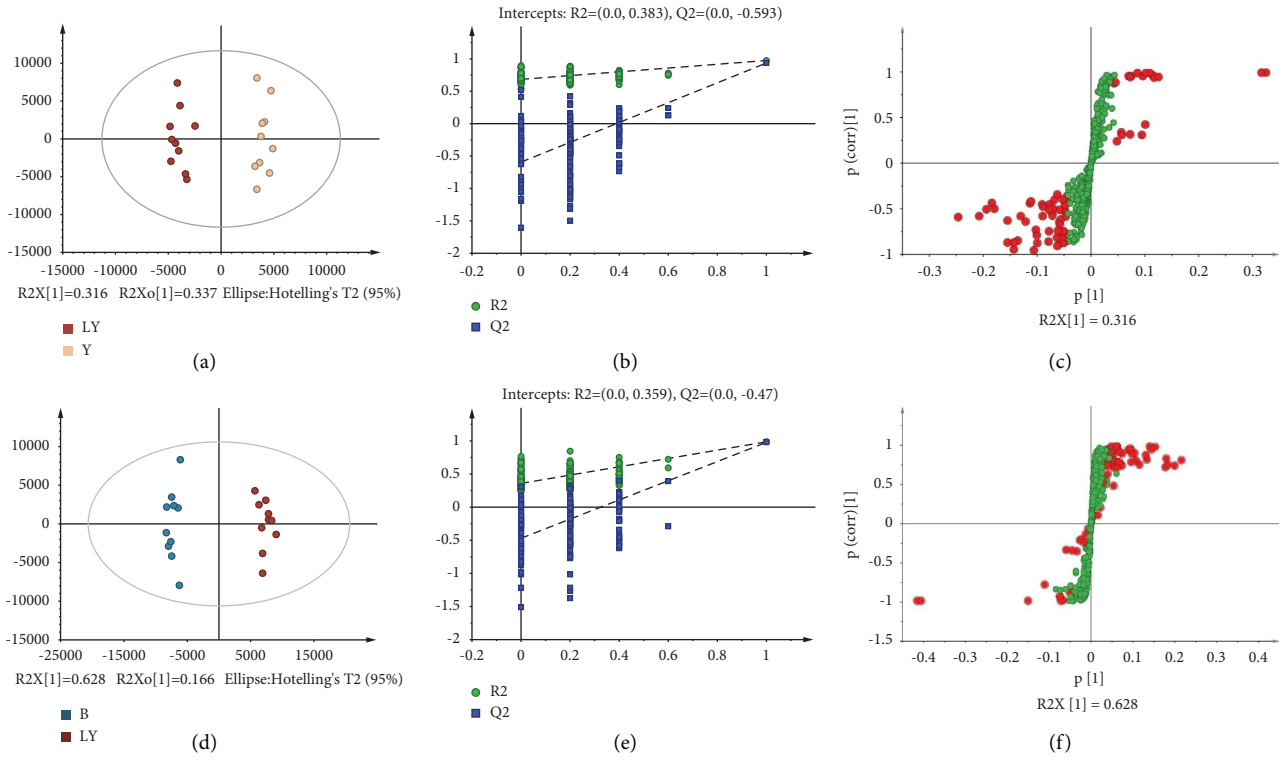


Figure 4: Continued.

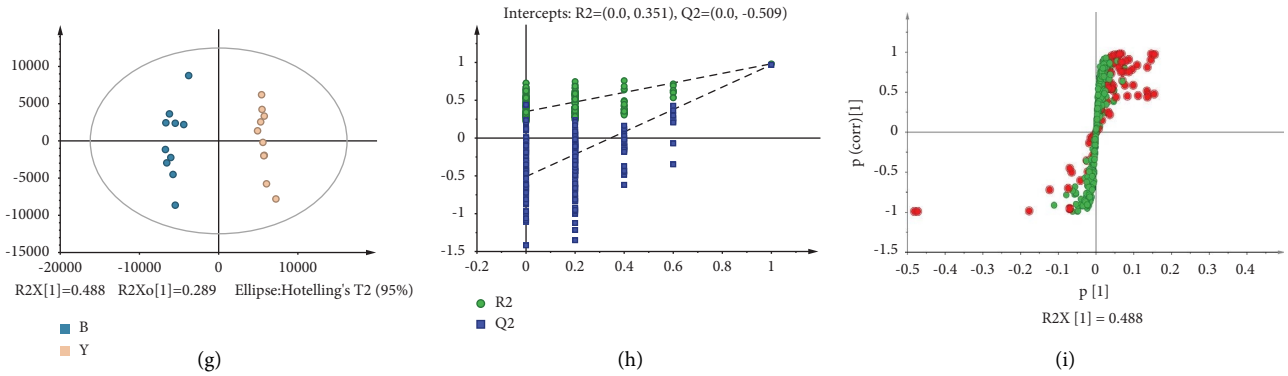


Figure 4: OPLS-DA score plots and the OPLS-DA permutation test and S-plot analysis of different levels of sf-CR: OPLS-DA score plot (a, d, g), permutation test plot of the OPLS-DA model (b, e, h), and S-plot (c, f, i).

deemed to be the primary VOCs responsible for the differences between the three levels of sf-CR. As a result, 20, 26, and 15 VOCs were filtered out from the light stir-fry vs. yellow group, light stir-fry vs. black group, and yellow vs. black group. When compared with the stir-frying lightly group, 14 VOCs in the yellow group decreased while 6 VOCs increased; furthermore, in the black group, 19 decreased and 7 increased. In addition, when compared to the yellow stir-fry group, 12 VOCs in the group black decreased, while 3 VOCs increased. Subsequently, after removing the repeated VOCs from the three groups, a total of 33 unique VOCs were identified.

3.3.2. Identification and Analysis of Differential Compounds. On the basis of the NIST 20.0 database, GC-MS postrun analysis was utilized to determine 33 key differential compounds. 21 sesquiterpenes, 8 monoterpene hydrocarbons, and 4 pyrazines were identified. The information included the compound name, RI, formula, category, molecular weight, as presented in Table 2 (the GC-MS raw data of differential compounds are shown in Table S3). Using a heat map (Figure 5(a)), we analyzed the distribution of the various compounds present in sf-CR samples of varying concentrations in order to determine their presence. Ten samples processed using the same method at three different levels of stir-frying were clustered into a single group, indicating excellent homogeneity among biological duplicates and high data reliability. In the various sf-CR samples, the accumulation of these compounds exhibited a distinct phenotypic variation with regard to their abundance.

Based on their accumulation patterns, these compounds could be clearly categorized into four major clusters. The relative concentration of components in clusters 1 and 4 increased with increasing degree of frying in all samples. On the other hand, the relative concentration of components in clusters 2 and 3 decreased as the degree of frying increased. Thus, it is possible that as stir-frying is intensified, the concentration of certain terpenoids decreases while the concentration of pyrazine rises. Notably, these pyrazine compounds were not reported in the CR study; however, they may be the new components of CR after stir-frying.

It is worth noting that aromatic herbs produce pyrazine compounds when fried. Apparently, it results from the Maillard reaction between amino acids and carbohydrates [45]. During roasting, the Maillard reaction occurs at relatively high temperatures and low levels of moisture. In the Maillard reaction, moisture is a crucial factor that determines the direction of the reaction and the quantity of volatile compounds produced via this pathway [46]. This is one reason that the aroma profiles of the roasted and boiled samples were distinct [47, 48]. With the extension of stir frying time, the moisture content in CR decreased, which promoted the occurrence of Maillard reaction. Consequently, as stir-frying intensifies, pyrazine levels rise. Terpenoids are highly volatile; however, in stir-frying processing, the temperature is elevated, and some components are susceptible to oxidative decomposition, rearrangement, isomerization, and other reactions, which will result in a reduction of terpenoids. Intriguingly, there is also an increase in the content of a small number of terpenoids, which we hypothesize may be the result of transformations between complex constituents that require further investigation.

3.4. Correlation Analysis of Differential VOCs and E-Nose Sensors. In addition to the above, we assessed the relationships between 33 key differential VOCs and the aroma of sf-CR using Spearman's rank correlation (Figure 5(b)). The results revealed that the differential compounds were most strongly correlated with sensors W3C, W5C, and W3S. These three sensors are activated by ammonia, aromatic compounds, and aromatic compounds, alkenes, respectively (Table 1). Of these, 2-methyl pyrazine (P1), 1,4-dimethylpyrazole (P2), 2,5-dimethylpyrazine (P3), 2-methoxy pyrazine (P4), D-limonene(P8), camphene (P9), trans-verbenol (P10), and pinocarvone (P11) had positive correlations with W3C and W5C response values and negative correlations with W3S. Other components, excluding p-cymene and copaene, exhibited a negative correlation with the response values of W3C and W5C but a positive correlation with W3S. These were the principal volatile flavor compounds present in sf-CR. As observed, these findings were consistent with the results of the differential

Table 2: Differential compounds between three levels of sf-CR.

NO.	Compounds	IUPAC name	RI	Ontology	Formula	Molecular weight
1	2-Methyl pyrazine	2-Methylpyrazine	469	Pyrazine	$C_5H_6N_2$	94.11
2	1,4-Dimethylpyrazole	1,4-Dimethylpyrazole	474	Pyrazole	$C_5H_8N_2$	96.13
3	2,5-Dimethyl pyrazine	2,5-Dimethylpyrazine	576	Pyrazine	$C_6H_8N_2$	108.14
4	2-Methoxy pyrazine	2-Methoxypyrazine	610	Pyrazine	$C_5H_6N_2O$	110.11
5	α-Pinene	2,6,6-Trimethylbicyclo [3.1.1]hept-2-ene	836	Monoterpene	$C_{10}H_{16}$	136.23
6	β-Pinene	(1S,5S)-2,6,6-Trimethylbicyclo [3.1.1]hept-2-ene	979	Monoterpene	$C_{10}H_{16}$	136.23
7	p-Cymene	1-Methyl-4-propan-2-ylbenzene	1026	Monoterpene	$C_{10}H_{14}$	134.22
8	D-Limonene	1-Methyl-4-prop-1-en-2-ylcyclohexene	1030	Monoterpene	$C_{10}H_{16}$	136.23
9	Camphene	2,2-Dimethyl-3-methylidenebicyclo[2.2.1]heptane	1130	Monoterpene	$C_{10}H_{16}$	136.23
10	Trans-verbenol	(1R,2S,5R)-4,6,6-Trimethylbicyclo[3.1.1]hept-3-en-2-ol	1147	Oxygenated monoterpene	$C_{10}H_{16}O$	152.23
11	Pinocarvone	6,6-Dimethyl-2-methylidenebicyclo[3.1.1]heptan-3-one	1158	Oxygenated monoterpene	$C_{10}H_{14}O$	150.22
12	(-)-Myrtenal	(1R,5S)-6,6-Dimethylbicyclo[3.1.1]hept-2-ene-2-carbaldehyde	1167	Oxygenated monoterpene	$C_{10}H_{14}O$	150.22
13	β-Vatirenene	(1R,8aS)-1,8a-Dimethyl-7-propan-2-ylidene-1.2,6,8-tetrahydronaphthalene	1173	Sesquiterpenoids	$C_{15}H_{22}$	202.33
14	Ylangene	(1S,2R,6R,7R,8S)-1,3-Dimethyl-8-propan-2-yltricyclo[4.4.0.02,7]dec-3-ene	1181	Sesquiterpenoids	$C_{15}H_{24}$	204.35
15	β-Elemene	(1S,2S,4R)-1-Ethenyl-1-methyl-2,4-bis(prop-1-en-2-yl)cyclohexane	1187	Sesquiterpenoids	$C_{15}H_{24}$	204.35
16	α-Guaiene	7-Isopropenyl-1,4-dimethyl-1,2,3,4,5.6,7,8-octahydroazulene	1191	Sesquiterpenoids	$C_{15}H_{24}$	204.35
17	Santalene	1,7-Dimethyl-7-(4-methylpent-3-enyl)tricyclo[2.2.1.02,6]heptane	1211	Sesquiterpenoids	$C_{15}H_{24}$	204.35
18	3,5,11-Eudesmatriene	5,8a-Dimethyl-3-prop-1-en-2-yl-2,3,7,8-tetrahydro-1H-naphthalene	1291	Sesquiterpenoids	$C_{15}H_{22}$	202.33
19	β-Humulene	(1E,5E)-1,4,4-Trimethyl-8-methylidenecycloundeca-1,5-diene	1293	Sesquiterpenoids	$C_{15}H_{24}$	204.35
20	(+)-Sativene	(1R,2S,3S,6S,8S)-6-Methyl-7-methylidene-3-propan-2-yltricyclo[4.4.0.02.8]decane	1301	Sesquiterpenoids	$C_{15}H_{24}$	204.35
21	α-Cubebene	(1R,5S,6R,7S,10R)-4,10-Dimethyl-7-isopropyltricyclo[4.4.0.01.5]deca-3-ene	1314	Sesquiterpenoids	$C_{15}H_{24}$	204.35
22	β-Gurjunene	(1aR,4R,4aR,7aR,7bR)-1,1,4-Trimethyl-7-methylidene-2,3,4,4a,5,6,7a,7b-octahydro-1aH-cyclopropa[e]azulene	1325	Sesquiterpenoids	$C_{15}H_{24}$	204.35
23	Copaene	(1R,2S,6S,7S,8S)-1,3-Dimethyl-8-propan-2-yltricyclo[4.4.0.02.7]dec-3-ene	1332	Sesquiterpenoids	$C_{15}H_{24}$	204.35
24	Cyperene epoxide	4,11,12,12-Tetramethyl-5-oxatetracyclo[6.3.1.01.6.04.6]dodecane	1340	Sesquiterpenoids	$C_{15}H_{24}O$	220.35
25	α-Calacorene	(1S)-4,7-Dimethyl-1-propan-2-yl-1,2-dihydronaphthalene	1344	Sesquiterpenoids	$C_{15}H_{20}$	200.32
26	(-)-Spathulenol	(1aR,4aR,7S,7aR,7bR)-1,1,7-Trimethyl-4-methylidene-1a,2,3,4a,5,6,7a,7b-octahydrocyclopropa[h]azulen-7-ol	1375	Sesquiterpenoids	$C_{15}H_{24}O$	220.35
27	Ledene oxide-(II)	3,7,7,10-Tetramethyl-2-oxatetracyclo[7.3.0.01,3.06,8]dodecane	1377	Sesquiterpenoids e	$C_{15}H_{24}O$	220.35
28	Caryophyllene oxide	(1R,4R,6R,10S)-4,12,12-Trimethyl-9-methylidene-5-oxatricyclo[8.2.0.04,6]dodecane	1386	Sesquiterpenoids	$C_{15}H_{24}O$	220.35
29	Caryophyllene (z-)	(1S,4Z,9S)-4,11,11-Trimethyl-8-methylidenebicyclo[7.2.0]undec-4-ene	1414	Sesquiterpenoids	$C_{15}H_{24}$	204.35
30	Isospathulenol	(1aR,7S,7aS,7bR)-1,1,4,7-Tetramethyl-2,3,5,6,7a,7b-hexahydro-1aH-cyclopropa[h]azulen-7-ol	1422	Sesquiterpenoids	$C_{15}H_{24}O$	220.35
31	Alloaromadendrene oxide-(2)	(1aR,4S,4aR,7R,7aS,7bS)-1,1,7-Trimethylspiro[2,3,4a,5,6,7,7a,7b-octahydro-1aH-cyclopropa[e]azulene-4,2′-oxirane]	1432	Sesquiterpenoids	$C_{15}H_{24}O$	220.35
32	Cyperotundone	(1R,7R,10R)-4,10,11,11-Tetramethyltricyclo[5.3.1.01,5]undec-4-en-3-one	1503	Sesquiterpenoids	$C_{15}H_{22}O$	218.33
33	α-Cyperone	(4aS,7R)-1,4a-Dimethyl-7-prop-1-en-2-yl-3,4,5,6,7,8-hexahydronaphthalen-2-one	1749	Sesquiterpenoids	$C_{15}H_{22}O$	218.33

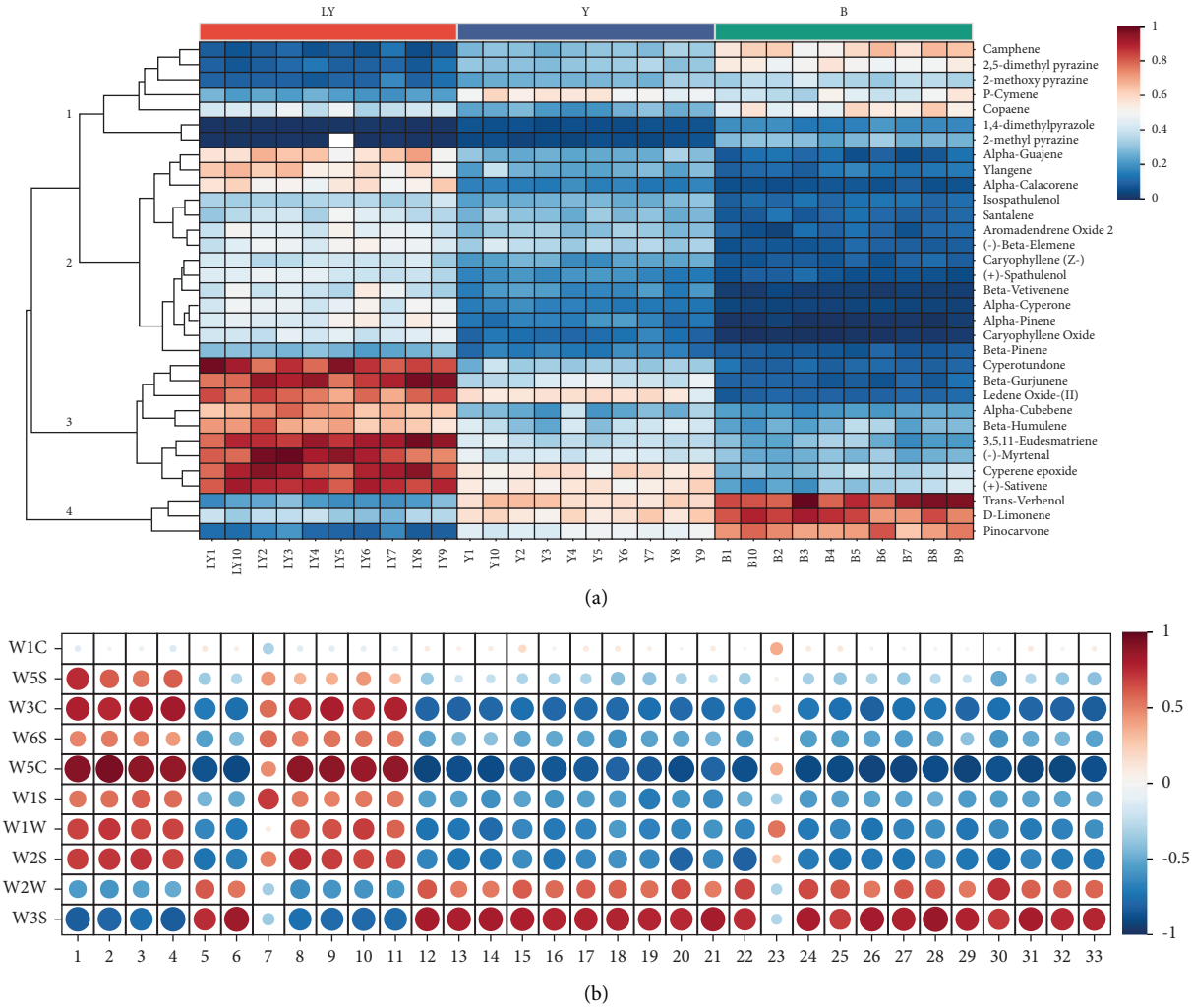


Figure 5: Heat map of differential compounds and correlation analysis chart of differential compounds with e-nose response: differential compound heat map (a). Correlation analysis chart (b). (The symbol "∗" indicates that the correlation coefficient is greater than 0.7).

component heat map. As the intensity of stir-frying increased, the proportion of pyrazines and a small amount of terpenoids (P8, P9, P10, and P11) increased, and the aroma intensified accordingly.

Based on correlation analysis, we found the main compounds that cause aroma differences. Pyrazines are nitrogen-containing heterocyclics characterized by their potency [49]. Due to their low vapor pressure, pyrazines readily evaporate [46]. Numerous of these substances have intense aromas and extremely low aroma threshold values [46]. Consequently, these compounds contribute to a variety of flavors. The results of this study revealed a direct correlation between sf-CR aroma and pyrazine content. In addition, it has been discovered that some pyrazines have pharmacological effects, including antithrombogenic, diuretic, and hepatoprotective [50–52]. In addition, numerous flavor volatiles have been derived from terpenoids unrelated to nutrients [53]. However, many of these terpenoids are also known to possess antimicrobial properties. These findings may, therefore, provide a foundation for future research on the application of sf-CR in food and medicine at varying concentrations.

4. Conclusion

In this study, an integrated method combining E-tongue, E-nose, and HS-GC-MS was developed for the first time in order to investigate the distinctions between three distinct levels of sf-CR. As the intensity of stir-frying increased, the flavor of sf-CR diminished while its aroma increased. Accordingly, the three types of sf-CR were screened for and identified with 33 distinct compounds, including 29 terpenoids and 4 pyrazines. The proportion of terpene components decreased as stir-frying intensity increased, while the proportion of pyrazine components increased. Additionally, Spearman's rank correlation allowed us to identify 2-methylpyrazine, 1,4-dimethylpyrazole, 2,5-dimethylpyrazine, 2-methoxypyrazine, D-limonene, camphene, trans-verbenol, and ponocarvone as the primary components causing aroma differences. Thus, the current study

established a method for identifying the differences in flavor, aroma, and volatile components of the three levels of sf-CR, as well as screening the major components responsible for aroma differences. This provides a reference for the use of sf-CR in food processing and medicine, as well as new ideas and methodologies for the investigation of other foods and pharmaceuticals.

Abbreviations

E-tongue: Electronic tongue
E-nose: Electronic nose
HS-GC-MS: Headspace gas chromatography-mass spectrometry
CR: *Cyperus rotundus*
sf-CR: Stir-frying process of *Cyperus rotundus*
VOCs: Volatile compounds
TCM: Traditional Chinese medicine
HCA: Hierarchical cluster analysis
PCA: Principal component analysis
OPLS-DA: Orthogonal partial least squares-discriminant analysis.

Data Availability

The data that support the findings of this study are available from the corresponding author upon reasonable request.

Conflicts of Interest

The authors declare that they have no conflicts of interest.

Authors' Contributions

Fengxia Wang and Qi Qian contributed equally to this work.

Acknowledgments

The Central Government supported this work by guiding Local Science and Technology Development Fund Projects (No. 206Z2501G), Hebei Provincial Key Research and Development Projects (No. 20372502D and 23372502D), and Natural Science Foundation of Hebei Province (No. H2019423050). This work was supported by the Natural Science Foundation of Hebei Province (Key Program) (Grant/Award Number: H2022423335).

Supplementary Materials

The experimental data of the electronic nose and electronic tongue are presented in the Supplementary Materials, Table S1, Table S2, and Table S3. (*Supplementary Materials*)

References

[1] State Pharmacopoeia Commission of the PRC, *Pharmacopoeia of the People's Republic of China (Volume I)*, People's Health Publishing House, Beijing, China, 2020.

[2] L. Guo, M. Gong, S. Wu, F. Qiu, and L. Ma, "Identification and quantification of the quality markers and anti-migraine active components in Chuanxiong Rhizoma and Cyperi Rhizoma herbal pair based on chemometric analysis between chemical constituents and pharmacological effects," *Journal of Ethnopharmacology*, vol. 246, Article ID 112228, 2020.

[3] F. Y. Wang, S. H. Zhang, J. X. Zhang, and F. Yuan, "Systematic review of ethnomedicine, phytochemistry, and pharmacology of Cyperi Rhizoma," *Frontiers in Pharmacology*, vol. 13, Article ID 965902, 2022.

[4] M. Yu, X. R. Zhang, C. C. Zhang et al., "Historical evolution and modern research of processing of cyperi rhizoma: a review," *Chinese Journal of Experimental Traditional Medical Formulae*, vol. 29, no. 03, pp. 223–232, 2023.

[5] *Introduction to Medicine*, China Traditional Chinese Medicine Publishing House, pp. 189–190, 1995.

[6] *Pharmaceutical Meaning*, China Traditional Chinese Medicine Publishing House, p. 29, 2012.

[7] F. X. Wang, Q. Qian, and B. L. Li, "Research progress on chemical constituents and pharmacological effects of Cyperi Rhizoma and predictive analysis of its quality marker (Q-Marker)," *Chinese Traditional and Herbal Drugs*, vol. 53, pp. 5225–5234, 2022.

[8] A. Hanifah, A. Maharijaya, S. P. Putri, W. A. Laviña, and Sobir, "Untargeted metabolomics analysis of eggplant (solanum melongena L.) fruit and its correlation to fruit morphologies," *Metabolites*, vol. 8, no. 3, p. 49, 2018.

[9] J. Yun, C. Cui, S. Zhang et al., "Use of headspace GC/MS combined with chemometric analysis to identify the geographic origins of black tea," *Food Chemistry*, vol. 360, Article ID 130033, 2021.

[10] D. M. Drexler, M. D. Reily, and P. A. Shipkova, "Advances in mass spectrometry applied to pharmaceutical metabolomics," *Analytical and Bioanalytical Chemistry*, vol. 399, no. 8, pp. 2645–2653, 2011 Mar.

[11] B. Wang, T. X. Zhang, Q. Zhao, X. C. Meng, Y. F. Li, and D. W. Zhao, "Application progress of metabonomics in medicinal plants," *Chinese Archives of Traditional Chinese Medicine*, vol. 39, no. 05, pp. 28–31, 2021.

[12] S. Sultana, M. Ali, and S. R. Mir, "Chemical constituents from the rhizomes of Cyperus rotundus L," *The Open Plant Science Journal*, vol. 10, no. 1, pp. 82–91, 2017.

[13] L. Kakarla, S. B. Katragadda, and M. Botlagunta, "Morphological and chemoprofile (liquid chromatography-mass spectroscopy and gas chromatography-mass spectroscopy) comparisons of Cyperus scariosus R. Br and Cyperus rotundus L," *Pharmacognosy Magazine*, vol. 11, pp. s439–s447, 2015.

[14] J. R. Lu, N. Xu, Y. Z. Mou, W. B. Li, C. M. Fu, and H. L. Chen, "Comparative study on chemical components of volatile oil of xiangfu (cyperi rhizoma) from different origins based on GC-MS fingerprint combining with chemometric method," *Chinese Archives of Traditional Chinese Medicine*, vol. 39, no. 12, pp. 106–111, 2021.

[15] L. Yi, N. Dong, S. Liu, Z. Yi, and Y. Zhang, "Chemical features of pericarpium citri reticulatae and pericarpium citri reticulatae viride revealed by GC-MS metabolomics analysis," *Food Chemistry*, vol. 186, pp. 192–199, 2015.

[16] M. H. Chen and T. C. Huang, "Volatile and nonvolatile constituents and antioxidant capacity of oleoresins in three taiwan citrus varieties as determined by supercritical fluid extraction," *Molecules*, vol. 21, no. 12, p. 1735, 2016.

[17] Z. Wang, C. Han, Y. Xu et al., "The role of prostate-specific antigen and multiparametric magnetic resonance imaging in the diagnosis of granulomatous prostatitis induced by intravesical Bacillus Calmette-Guérin vaccine therapy in patients with nonmuscle invasive bladder cancer," *Journal of*

Cancer Research and Therapeutics, vol. 17, no. 3, pp. 625–629, 2021.

[18] J. M. Fang and W. X. Du, "Material basis research of oour properties and five flavors of traditional Chinese medicine," *Ournal of Liaoning University of Traditional Chinese Medicine*, vol. 17, no. 12, pp. 66–68, 2015.

[19] X. R. Gui, J. L. Shen, and L. X. Wei, "Analysis on the construction of five flavours cultural cognitive theories of traditional Chinese medicine from the perspective of embodied cognition," *China Journal of Traditional Chinese Medicine and Pharmacy*, vol. 36, pp. 3887–3889, 2021.

[20] X. Q. Li, Y. H. Yang, Y. T. Zhu, A. L. Ben, and J. Qi, "A novel strategy for discriminating different cultivation and screening odor and taste flavor compounds in Xinhui tangerine peel using E-nose, E-tongue, and chemo metrics," *Food Chemistry*, vol. 384, Article ID 132519, 2022.

[21] Z. Duan, S. Dong, Y. Dong, and Q. Gao, "Geographical origin identification of two salmonid species via flavor compound analysis using headspace-gas chromatography-ion mobility spectrometry combined with electronic nose and tongue," *Food Research International*, vol. 145, Article ID 110385, 2021.

[22] Z. Haddi, S. Mabrouk, M. Bougrini et al., "E-Nose and e-Tongue combination for improved recognition of fruit juice samples," *Food Chemistry*, vol. 150, pp. 246–253, 2014.

[23] M. Xu, S. L. Yang, W. Peng et al., "A novel method for the discrimination of semen arecae and its processed products by using computer vision, electronic nose, and electronic tongue," *Evid Based Complement Alternat Med*, vol. 2015, Article ID 753942, 10 pages, 2015.

[24] D. Luo, H. Zhou, H. Gholamhosseini et al., "Aroma characteristic analysis of Amomi fructus from different habitats using machine olfactory and gas chromatography-mass spectrometry," *Pharmacognosy Magazine*, vol. 15, no. 63, p. 392, 2019.

[25] J. J. Ding, C. M. Gu, L. F. Huang, and R. Tan, "Discrimination and geographical origin prediction of cynomorium songaricum rupr. From different growing areas in China by an electronic tongue," *Journal of Analytical Methods in Chemistry*, vol. 2018, Article ID 5894082, 6 pages, 2018.

[26] X. Y. Yin, Y. C. Lv, R. X. Wen, Y. Wang, Q. Chen, and B. H. Kong, "Characterization of selected Harbin red sausages on the basis of their flavour profiles using HS-SPME-GC/MS combined with electronic nose and electronic tongue," *Meat Science*, vol. 172, Article ID 108345, 2021.

[27] S. Z. Li, S. L. Zeng, Y. Wu et al., "Cultivar differentiation of Citri Reticulatae Pericarpium by a combination of hierarchical three-step filtering metabolomics analysis, DNA barcoding and electronic nose," *Analytica Chimica Acta*, vol. 1056, pp. 62–69, 2019.

[28] Intelligent Sensor Technology, *Taste Sensing System User's Guide First Edition*, Intelligent Sensor Technology, Kanagawa, Japan, 2012.

[29] Y. Tahara and K. Toko, "Electronic tongues-A review," *IEEE Sensors Journal*, vol. 13, no. 8, pp. 3001–3011, 2013.

[30] Z. Li, H. Zhou, D. H. Luo, H. Gholamhosseini, B. Han, and H. X. Wang, "Rapid qualitative and quantitative analysis of volatile components and quality identification of amomi fructus based on bionic olfactory system," *Pharmacognosy Magazine*, vol. 17, no. 74, p. 223, 2021.

[31] H. Tsugawa, T. Cajka, T. Kind et al., "MS-DIAL: data-independent MS/MS deconvolution for comprehensive metabolome analysis," *Nature Methods*, vol. 12, no. 6, pp. 523–526, 2015.

[32] T. Zeng, B. H. Fang, F. L. Huang et al., "Mass spectrometry-based metabolomics investigation on two different indica rice grains (Oryza sativa L.) under cadmium stress," *Food Chemistry*, vol. 343, Article ID 128472, 2021.

[33] Z. K. Chen, H. Y. Chen, Y. Jiang et al., "Metabolomic analysis reveals metabolites and pathways involved in grain quality traits of high-quality rice cultivars under a dry cultivation system," *Food Chemistry*, vol. 326, Article ID 126845, 2020.

[34] X. X. Cao, L. L. Sun, D. Li, G. J. You, M. Wang, and X. L. Ren, "Quality evaluation of phellodendri chinensis cortex by fingerprint-chemical pattern recognition," *Molecules*, vol. 23, no. 9, p. 2307, 2018.

[35] P. Y. Wang, Y. H. Fang, Q. Guo, J. Zhang, X. Ling, and H. Yang, "Metabolomics analysis of hairy roots of endangered Mongolian medicine Ammopiptanthus mongolicus," *Natural Product Research and Development*, vol. 34, pp. 647–655, 2022.

[36] K. Zhang, J. Su, Y. T. Huang et al., "Untargeted metabolomics reveals the synergistic mechanisms of Yuanhu Zhitong oral liquid in the treatment of primary dysmenorrhea," *Journal of Chromatography B*, vol. 1165, Article ID 122523, 2021.

[37] D. Pu, Y. Shan, L. Zhang, B. Sun, and Y. Zhang, "Identification and inhibition of the key off-odorants in duck broth by means of the sensomics approach and binary odor mixture," *Journal of Agricultural and Food Chemistry*, vol. 70, no. 41, pp. 13367–13378, 2022.

[38] Y. Kobayashi, M. Habara, H. Ikezazki, R. Chen, Y. Naito, and K. Toko, "Advanced taste sensors based on artificial lipids with global selectivity to basic taste qualities and high correlation to sensory scores," *Sensors*, vol. 10, no. 4, pp. 3411–3443, 2010.

[39] W. G. Jing, Q. Zhang, X. L. Cheng, J. Shi, S. C. Ma, and F. Wei, "Discussion on the processing mechanism of ginger Magnoliae officinalis cortex based on electronic nose and tongue technology," *Hebei Journal of Industrial Science and Technology*, vol. 38, pp. 414–422, 2021.

[40] P. K. Kimes, Y. Liu, D. Neil Hayes, and J. S. Marron, "Statistical significance for hierarchical clustering," *Biometrics*, vol. 73, no. 3, pp. 811–821, 2017.

[41] N. Anjiki, J. Hosoe, H. Fuchino et al., "Evaluation of the taste of crude drug and Kampo formula by a taste-sensing system (4): taste of Processed Aconite Root," *Journal of Natural Medicines*, vol. 65, no. 2, pp. 293–300, 2011.

[42] R. Jayasundar and S. Ghatak, "Spectroscopic and E-tongue evaluation of medicinal plants: a taste of how rasa can be studied," *Journal of Ayurveda and Integrative Medicine*, vol. 7, no. 4, pp. 191–197, 2016.

[43] W. X. Wang and W. X. Du, "Traditional Chinese medicine (TCM) four gas mixed theory and correlation analysis," *Chinese Journal of Ethnomedicine and Ethnopharmacy*, vol. 26, no. 24, pp. 61–63, 2017.

[44] C. Kang, Y. Zhang, M. Zhang et al., "Screening of specific quantitative peptides of beef by LC-MS/MS coupled with OPLS-DA," *Food Chemistry*, vol. 387, Article ID 132932, 2022.

[45] H. I. Hwang, T. G. Hartman, R. T. Rosen, and C. T. Ho, "Formation of pyrazines from the Maillard reaction of glucose and glutamine-amide-15N," *Journal of Agricultural and Food Chemistry*, vol. 41, no. 11, pp. 2112–2115, 1993.

[46] R. Müller and S. Rappert, "Pyrazines: occurrence, formation and biodegradation," *Applied Microbiology and Biotechnology*, vol. 85, no. 5, pp. 1315–1320, 2010.

[47] T. Shibamoto and R. A. Bernhard, "Investigation of pyrazine formation pathways in glucose-ammonia model systems," *Agricultural and Biological Chemistry*, vol. 41, no. 1, pp. 143–153, 1977.

[48] S. Bi, A. Wang, Y. Wang et al., "Effect of cooking on aroma profiles of Chinese foxtail millet (Setaria italica) and correlation with sensory quality," *Food Chemistry*, vol. 289, pp. 680–692, 2019.

[49] G. J. Richards and J. P. Hill, "The pyrazinacenes," *Accounts of Chemical Research*, vol. 54, no. 16, pp. 3228–3240, 2021.

[50] J. H. Jones, J. B. Bicking, and E. J. Cragoe Jr, "Pyrazine diuretics. IV. N-amidino-3-amino-6-substituted pyrazinecarboxamides," *Journal of Medicinal Chemistry*, vol. 10, no. 5, pp. 899–903, 1967.

[51] N. D. Kim, M. K. Kwak, and S. G. Kim, "Inhibition of cytochrome P450 2E1 expression by 2-(allylthio)pyrazine, a potential chemoprotective agent: hepatoprotective effects," *Biochemical Pharmacology*, vol. 53, no. 3, pp. 261–269, 1997.

[52] X. Lian, S. Wang, G. Xu, N. Lin, Q. Li, and H. Zhu, "The application with tetramethyl pyrazine for antithrombogenicity improvement on silk fibroin surface," *Applied Surface Science*, vol. 255, no. 2, pp. 480–482, 2008.

[53] S. A. Goff and H. J. Klee, "Plant volatile compounds: sensory cues for health and nutritional value," *Science*, vol. 311, no. 5762, pp. 815–819, 2006.